

SUPPLEMENTARY INFORMATION

Confinement of β -barrel proteins in nanoporated free-standing nanomembranes for ion transport

Anna Puiggali-Jou,^{1,2} Maria M. Pérez-Madrigal,^{1,2,*} Luis J. del Valle,^{1,2} Elaine
Armelin,^{1,2} María T. Casas,¹ Catherine Michaux,³ Eric A. Perpète,³ Francesc Estrany,^{2,4}
and Carlos Alemán^{1,2,*}

¹ *Departament d'Enginyeria Química, ETSEIB, Universitat Politècnica de Catalunya,
Avda. Diagonal 647, Barcelona E-08028, Spain*

² *Center for Research in Nano-Engineering, Universitat Politècnica de Catalunya,
Campus Sud, Edifici C', C/Pasqual i Vila s/n, Barcelona E-08028, Spain*

³ *Laboratoire de Chimie Physique des Biomolécules, Unité de Chimie Physique
Théorique et Structurale (UCPTS), University of Namur,
Rue de Bruxelles, 61, 5000 Namur, BELGIUM.*

⁴ *Departament d'Enginyeria Química, Escola Universitària d'Enginyeria Tècnica
Industrial de Barcelona, Universitat Politècnica de Catalunya, Comte d'Urgell 187,
08036 Barcelona, Spain*

METHODS

Materials

PLA, a product of Natureworks (polymer 2002D), was supplied by Nupik International (Polinyà, Spain). According to the manufacturer, this PLA has a D content of 4.25%, a residual monomer content of 0.3%, density of 1.24 g/cm³, glass transition temperature of 58 °C, and melting point of 153 °C. The number and weight average molecular weight is $M_n=98,100$ g/mol and $M_w=181,000$ g/mol, respectively. PVA (87-89% hydrolysed) with $M_w=13,000 - 23,000$ g/mol was purchased from Sigma-Aldrich (USA). Dry trichloromethane stabilized with 50 ppm of amylene DS-ACS (99.9%) was purchased from Panreac Quimica S.A.U. (Spain). 1,1,1,3,3,3-Hexafluoroisopropanol (HFIP) was purchased from Apollo Scientific Limit (UK). SiO₂ cover-glasses of 14 mm of diameter were acquired from Agar Scientific (France), while indium tin oxide coated glass slides with surface resistivity of 15-25 Ω/sq and dimensions of 75 × 25 × 1.1 mm³ were obtained from Sigma-Aldrich. Ultrapure milliQ water was used to prepare all the aqueous solutions.

Expression, purification and refolding of the Omp2a outer membrane protein from Brucella Melitensis

Bacterial Strain and Growth. Cells of *E. coli* BL21 (DE3) carrying pLysS and pET2a plasmids (containing the gene Omp2a without peptide signal) were grown in LB medium at 37°C with constant shaking. Log cultures (OD 0.6) of 500 mL were stimulated with IPTG (0.2 mg mL⁻¹) for 3 h. Cells were then harvested by centrifugation at 4,000 g for 30 min, and the resulting bacterial pellets were stored at -20°C.

Overexpression and Non-Native Purification of Omp2a. The bacterial pellets were thawed and treated with 8 mL of TEN lysis buffer (50 mM Tris-HCl pH 8, 1 mM

EDTA, 17 mM NaCl, 125 mM PMSF, 250 mg mL⁻¹ lysozyme) for 20 min at 25°C. Harvested cells were further broken by addition of 10 mg of sodium deoxycholate for 60 min at 37°C with constant shaking, and 2 mg of DNase I for 60 min at 25°C. The suspension was then centrifuged at 14,000 g for 20 min at 4°C. The resulting pellet underwent a washing buffer (2 M urea, 20 mM Tris-HCl pH 8, 500 mM NaCl, 2% Triton X-100) and centrifuged at 14,000 g for 20 min at 4°C. The inclusion bodies were solubilized with 8 mL of TEN buffer (50 mM Tris-HCl pH 8, 1 mM EDTA, 17 mM NaCl, 8 M urea). The solubilized proteins were then applied onto an anion-exchange DEAE column previously equilibrated with 25 mL of buffer (50 mM Tris-HCl pH 8, 17 mM NaCl, 8 M urea). Omp2a was eluted with a 50 mL linear gradient of NaCl from 17 to 500 mM, whereas the protein profile was further analyzed using SDS-PAGE. Fractions containing 39 kDa proteins were then pooled and stored at 4°C.

Omp2a Refolding in SDS-MPD System. To refold Omp2a, the protein solution (1 mg mL⁻¹ protein, 250 mM NaCl, 50 mM Tris-HCl pH 8, and 8 M urea) was eluted onto a PD-10 column to exchange the buffer (150 mM NaCl, 50 mM Tris-HCl pH 8, and 120 mM SDS – where SDS is sodium dodecyl sulfate –, which is 15 times the critical micellar concentration). SDS-unfolded samples were then diluted 1:1 in a refolding solution (50 mM Tris-HCl pH 8, 150 mM NaCl, 3 M MPD, where MDP is 2-methyl-2,4-pentanediol). The protein solution was then incubated at room temperature. The samples were stored at -20°C to stop the refolding reaction. Hereafter, Omp2a protein at this procedure stage is named as obtained Omp2a.

Sodium dodecyl sulfate polyacrylamide gel electrophoresis (SDS-PAGE)

Samples were loaded on 15% acrylamide SDS–PAGE gels without boiling. After electrophoresis, the gels were fixed with glacial acetic acid and methanol and stained with Coomassie blue.

Dynamic light scattering (DLS)

The size distribution of the protein in 1× PBS pH 7.4 and in 50 mM Tris–HCl pH 8, 150 mM NaCl, 3 M MPD was determined using a NanoBrook Omni Zeta Potential Analyzer from Brookhaven Instruments Corporation. Particularly, three consecutive runs of 60 seconds each were conducted for every sample.

Circular dichroism (CD)

CD spectra were recorded between 190 and 350 nm at room temperature using a Jasco J-815 equipment with a protein concentration of approximately 125 µg/mL and a 0.1 cm cell path. Spectra were acquired at a scan speed of 50 nm min⁻¹ with a 0.2 nm data pitch using a 2 nm bandwidth and a 4 second digital integration time. Spectra were averaged after two accumulations and corrected by subtraction of the background spectrum.

Transmission electron microscopy (TEM)

TEM images were obtained with a Philips TECNAI 10 electron microscope operating at 100 kV. Bright field micrographs were taken with an SIS MegaView II digital camera. Solution containing Omp2a (0.34 mg/mL) was dispersed on glow-discharged carbon coated copper grids (300 mesh) and negatively stained with uranyl acetate (2.0 % w/v). After incubation (30 s), the excess of protein was removed with filter paper, and the grids air dried for a further 1-2 s.

Preparation of nanoporated free-standing nanomembranes (FSNMs)

Nanoporated PLA FSNMs were prepared by applying the procedure described by Puiggali-Jou *et al.*¹. Firstly, a PVA solution in milliQ water (100 mg/mL) was spin-coated onto a clean glass slip or ITO substrate at 2500 rpm for 60 s to obtain a sacrificial layer. Before using, substrates were cleaned by successive sonication in acetone, ethanol and water (5 min) and dried with clean dry air. After this, a PLA:PVA solution with 90:10 or 99:1 v/v ratio, which was obtained by mixing PLA (10 mg/mL) and PVA (10 mg/mL) HFIP solutions and stirring vigorously (three times at 1000 rpm for 30 s each one using a Vortex-type mixer), was spin-coated at 7000 rpm for 60 s. Finally, the substrate coated with the PLA-PVA NM was immersed into milliQ water for separation of the NM from the substrate (*i.e.* dissolution of the sacrificial layer) as well as for the creation of the nanoporations (*i.e.* dissolution of PVA phases in PLA-PVA NMs).

Omp2a-filled nanoporated nanomembranes

Nanoporated PLA nanomembranes supported on ITO were placed in a 24-well plate. 500 μ L of Omp2a solutions (0.5, 0.25 and 0.125 mg/mL) were deposited onto the film surface. After 48 h with slight agitation (80 rpm) at room temperature, the nanomembranes surfaces were rinsed three times with milliQ water to remove non-immobilized protein residues.

Omp2a-coated non-perforated nanomembranes

Non-perforated PLA NMs were incubated in 500 μ L of Omp2a solution (0.5 mg/mL) for 48 h with slight agitation (80 rpm) and at room temperature. After such period of time, samples were rinsed three times with milliQ water to remove non-immobilized

protein residues. The resulting Omp2a-coated non-perforated NMs were used as negative control.

Detection of immobilized protein: Bradford method

Adsorbed Omp2a was removed from the films surfaces by adding 0.2 mL of 0.1 M PBS with nonyl phenoxyethoxyethanol (NP-40) surfactant (0.5% v/v) and orbital shaking at 50 rpm during 30 min and 37°C. In order to avoid interferences between the NP40 surfactant and the Bradford reagent, the former was eliminated by precipitating the Omp2a with 20 µL of trichloroacetic acid. Next, the precipitate-containing solution was centrifuged for 15 min at 12000 rpm. The solid (Omp2a) was washed with cold acetone and maintained at 4 °C for 1 hour. After this, the solid was centrifuged again during 15 min at 12000 rpm. The protein was dried under vacuum and, finally, dissolved in 0.1 M PBS for Bradford assay.

Standard curves were carried out using protein dilutions, which were prepared using buffer solution with concentrations of protein ranging from 0.05 to 1.00 mg/mL. Next, 5 µL of protein standards and samples were added to a 96-well plate, blank wells being filled with 5µL of buffer. After this, Bradford reagent (250 µL) was added into each well and plates were subsequently placed on a shaker for mixing (30 s). Samples were incubated at room temperature for 15 min. Finally, the absorbance was measured at 595 nm.

Profilometry

Film thickness measurements were carried out using a Dektak 150 stylus profilometer (Veeco, Plainview, NY). Different scratches were intentionally provoked on the NMs and measured to allow statistical analysis of data. At least six independent

measurements were performed for two samples of each examined condition. Imaging of the films profile was conducted using the following optimized settings: tip radius= 12.5 μm ; stylus force= 3.0 mg; scan length= 3 mm; and speed= 30 $\mu\text{m/s}$.

Atomic Force Microscopy (AFM)

AFM was conducted to obtain topographic images of the films surface using silicon TAP 150-G probes (Budget Sensors, Bulgaria) with a frequency of 150 kHz and a force constant of 5 N/m. Images were obtained with an AFM Dimension microscope using a NanoScope IV controller under ambient conditions in tapping mode. The row scanning frequency was set between 0.6 and 0.8 Hz. The root mean square roughness (R_q), which is the average height deviation taken from the mean data plane, was determined considering $5 \times 5 \mu\text{m}^2$ surface areas and using the statistical application of the NanoScope Analysis software (1.20, Veeco). AFM measurements were performed on various parts of the films, which produced reproducible images similar to those displayed in this work.

Scanning electron microscopy (SEM)

SEM micrographs were obtained using a Focussed Ion Beam Zeiss Neon 40 scanning electron microscope operating at 1 kV. Samples were mounted on a double-side adhesive carbon disc and sputter-coated with a thin layer of carbon to prevent sample charging problems.

Wettability

Contact angle (CA) measurements were conducted using the water drop method. 0.5 μL of milliQ water drops were deposited onto the surface of the films and recorded after

stabilization with the equipment OCA 15EC (DataPhysics Instruments GmbH, Filderstadt). The SCA20 software was used to measure the CA, which is shown in this work as the average of at least 10 measures for each condition.

Electrochemical Impedance Spectroscopy (EIS)

EIS measurements were performed using a conventional three-electrode cell and an AUTOLAB-302N potentiostat/galvanostat operating between the frequency range of $10^{4.5}$ Hz and 10^{-2} Hz and 5 mV of amplitude for the sinusoidal voltage. All experiments were performed at room temperature with nanomembranes deposited onto ITO and using different electrolyte solutions (NaCl, KCl and CaCl₂) at various concentrations (50, 100, 500 and 1000 mM). ITO was used as working-electrode and platinum as counter-electrode, whereas Ag|AgCl saturated (KCl 3M) was employed as reference electrode. After data collection, EIS results were then processed and fitted to an electrical equivalent circuit (EEC).

1. A. Puiggalí-Jou, J. Medina, L. J. del Valle and C. Alemán, *Eur. Polym. J.*, 2016, **75**, 552-564.

Table S1. Accepted sequence (triple letter code) of Omp2a protein (367 amino acids).

Met - Asn - Ile - Lys - Ser - Leu - Leu - Leu - Gly - Ser - Ala - Ala - Ala - Leu - Val -
Ala - Ala - Ser - Gly - Ala - Gln - Ala - Ala - Asp - Ala - Ile - Val - Ala - Pro - Glu - Pro
- Glu - Ala - Val - Glu - Tyr - Val - Arg - Val - Cys - Asp - Ala - Tyr - Gly - Ala - Gly -
Tyr - Phe - Tyr - Ile - Pro - Gly - Thr - Glu - Thr - Cys - Leu - Arg - Val - His - Gly -
Tyr - Val - Arg - Tyr - Asp - Val - Lys - Gly - Gly - Asp - Asp - Val - Tyr - Ser - Gly -
Thr - Asp - Arg - Asn - Gly - Trp - Asp - Lys - Gly - Ala - Arg - Phe - Ala - Leu - Met -
Phe - Asn - Thr - Asn - Ser - Glu - Thr - Glu - Leu - Gly - Thr - Leu - Gly - Thr - Tyr -
Thr - Gln - Leu - Arg - Phe - Asn - Tyr - Thr - Ser - Asn - Asn - Ser - Arg - His - Asp -
Gly - Gln - Tyr - Gly - Asp - Phe - Ser - Asp - Asp - Arg - Asp - Val - Ala - Asp - Gly -
Gly - Val - Ser - Thr - Gly - Thr - Asp - Leu - Gln - Phe - Ala - Tyr - Ile - Thr - Leu -
Gly - Gly - Phe - Lys - Val - Gly - Ile - Asp - Glu - Ser - Glu - Phe - His - Thr - Phe -
Thr - Gly - Tyr - Leu - Gly - Asp - Val - Ile - Asn - Asp - Asp - Val - Val - Ala - Ala -
Gly - Ser - Tyr - Arg - Thr - Gly - Lys - Ile - Ala - Tyr - Thr - Phe - Thr - Gly - Gly -
Asn - Gly - Phe - Ser - Ala - Val - Ile - Ala - Leu - Glu - Gln - Gly - Gly - Glu - Asp -
Val - Asp - Asn - Asp - Tyr - Thr - Ile - Asp - Gly - Tyr - Met - Pro - His - Val - Val -
Gly - Gly - Leu - Lys - Tyr - Ala - Gly - Gly - Trp - Gly - Ser - Ile - Ala - Gly - Val -
Val - Ala - Tyr - Asp - Ser - Val - Ile - Glu - Glu - Trp - Ala - Thr - Lys - Val - Arg -
Gly - Asp - Val - Asn - Ile - Thr - Asp - Arg - Phe - Ser - Val - Trp - Leu - Gln - Gly -
Ala - Tyr - Ser - Ser - Ala - Ala - Thr - Pro - Asn - Gln - Asn - Tyr - Gly - Gln - Trp -
Gly - Gly - Asp - Trp - Ala - Val - Trp - Gly - Gly - Ala - Lys - Phe - Ile - Ala - Pro -
Glu - Lys - Ala - Thr - Phe - Asn - Leu - Gln - Ala - Ala - His - Asp - Asp - Trp - Gly -
Lys - Thr - Ala - Val - Thr - Ala - Asn - Val - Ala - Tyr - Gln - Leu - Val - Pro - Gly -
Phe - Thr - Ile - Thr - Pro - Glu - Val - Ser - Tyr - Thr - Lys - Phe - Gly - Gly - Glu -
Trp - Lys - Asp - Thr - Val - Ala - Glu - Asp - Asn - Ala - Trp - Gly - Gly - Ile - Val -
Arg - Phe - Gln - Arg - Ser - Phe

Table S2. Resistances (R) and constant phase elements (CPE) for each sample from fitting parameters obtained with the EEC displayed in Figure 5e. For each system impedance parameters are displayed according to the NaCl concentrations of 50, 100, 500 and 1000 mM. The percentage errors associated to each circuit element have been included in parentheses.

	R_S ($\Omega \cdot \text{cm}^2$)	CPE_M ($\text{Fcm}^{-2} \cdot \text{s}^{n-1}$)	n	R_M ($\Omega \cdot \text{cm}^2$)	CPE_{dl} ($\text{Fcm}^{-2} \cdot \text{s}^{n-1}$)	n	R_I ($\Omega \cdot \text{cm}^2$)
50 mM							
Non-perforated PLA	127.8 (1.5)	$2.91 \cdot 10^{-6}$ (3.6)	0.9 (0.9)	$12.3 \cdot 10^3$ (4.7)	$1.22 \cdot 10^{-5}$ (1.2)	0.21 (1.2)	$429 \cdot 10^3$ (2.7)
Nanoperforated PLA	99.9 (1.6)	$2.95 \cdot 10^{-5}$ (4.1)	0.56 (1.0)	$2.22 \cdot 10^3$ (4.8)	$6.14 \cdot 10^{-5}$ (1.1)	0.7 (1.1)	$33.7 \cdot 10^3$ (1.6)
Omp2a-filled nanoperforated PLA	98.9 (1.9)	$1.45 \cdot 10^{-5}$ (8.5)	0.95 (2.1)	$1.06 \cdot 10^3$ (4.6)	$5.1 \cdot 10^{-4}$ (5.4)	0.49 (2.5)	$5.1 \cdot 10^3$ (5.9)
100 mM							
Non-perforated PLA	133.2 (1.6)	$4.88 \cdot 10^{-6}$ (5.6)	0.85 (1.1)	$6.88 \cdot 10^3$ (6.6)	$1.18 \cdot 10^{-5}$ (1.3)	0.85 (1.2)	$443 \cdot 10^3$ (3.2)
Nanoperforated PLA	66.2 (1.4)	$2.66 \cdot 10^{-5}$ (3.6)	0.56 (0.8)	$2.63 \cdot 10^3$ (4.9)	$6.14 \cdot 10^{-5}$ (1.3)	0.7 (1.4)	$31.6 \cdot 10^3$ (1.9)
Omp2a-filled nanoperforated PLA	93.7 (1.4)	$1.49 \cdot 10^{-5}$ (5.9)	0.94 (1.6)	$1.49 \cdot 10^3$ (3.6)	$5.77 \cdot 10^{-4}$ (5.6)	0.54 (2.8)	$4.76 \cdot 10^3$ (5.4)
500 mM							
Non-perforated PLA	56 (1.1)	$3.15 \cdot 10^{-6}$ (4.7)	0.92 (1.2)	$5.99 \cdot 10^3$ (5.4)	$1.54 \cdot 10^{-5}$ (1.2)	0.79 (1.2)	$135.5 \cdot 10^3$ (1.9)

Nanoperforated PLA	36.9 (1.9)	$6.41 \cdot 10^{-5}$ (5.3)	0.51 (1.2)	883 (4.8)	$6.56 \cdot 10^{-5}$ (0.8)	0.75 (0.8)	$26.8 \cdot 10^3$ (1.2)
Omp2a-filled nanoperforated PLA	56.1 (1.9)	$2.46 \cdot 10^{-5}$ (13.1)	0.96 (2.9)	317 (6.2)	$7.54 \cdot 10^{-4}$ (3.1)	0.48 (2.3)	$4.49 \cdot 10^3$ (6.4)
1000 mM							
Non-perforated PLA	45.7 (1.4)	$4.03 \cdot 10^{-6}$ (8.0)	0.95 (1.8)	$2.59 \cdot 10^3$ (7.3)	$1.59 \cdot 10^{-5}$ (1.1)	0.77 (1.0)	$124.6 \cdot 10^3$ (1.8)
Nanoperforated PLA	26.66 (2.1)	$1.52 \cdot 10^{-4}$ (4.8)	0.43 (1.2)	669 (5.1)	$6.67 \cdot 10^{-5}$ (0.54)	0.77 (0.5)	$25.25 \cdot 10^3$ (0.8)
Omp2a-filled nanoperforated PLA	45.6 (2.4)	$3.88 \cdot 10^{-5}$ (23.5)	0.97 (5.2)	150.9 (11.4)	$7.25 \cdot 10^{-3}$ (8.0)	0.49 (2.5)	$5.14 \cdot 10^3$ (8.0)

Table S3. Resistances (R) and constant phase elements (CPE) for each sample from fitting parameters obtained with the EEC displayed in Figure 5e. For each system impedance parameters are displayed according to the KCl concentrations of 50, 100, 500 and 1000 mM. The percentage errors associated to each circuit element have been included in parentheses.

	$R_S (\Omega \cdot \text{cm}^2)$	$CPE_M (\text{Fcm}^{-2} \cdot \text{s}^{n-1})$	n	$R_M (\Omega \cdot \text{cm}^2)$	$CPE_{dl} (\text{Fcm}^{-2} \cdot \text{s}^{n-1})$	n	$R_I (\Omega \cdot \text{cm}^2)$
50 mM							
Non-perforated PLA	184.4 (1.9)	$5.68 \cdot 10^{-6}$ (6.6)	0.8 (1.3)	$6.16 \cdot 10^3$ (6.0)	$1.04 \cdot 10^{-5}$ (1.3)	0.93 (1.0)	$492 \cdot 10^3$ (2.9)
Nanoperforated PLA	74.4 (2.6)	$3 \cdot 10^{-5}$ (8.2)	0.53 (1.8)	$1.58 \cdot 10^3$ (6.8)	$5.67 \cdot 10^{-5}$ (1.5)	0.72 (1.5)	$37.7 \cdot 10^3$ (2.6)
Omp2a-filled nanoperforated PLA	110.5 (2.6)	$1.62 \cdot 10^{-5}$ (8.4)	0.83 (2.8)	$2.2 \cdot 10^3$ (7.3)	$4.65 \cdot 10^{-4}$ (16.7)	0.51 (4.9)	$3.56 \cdot 10^3$ (8.1)
100 mM							
Non-perforated PLA	107.2 (1.5)	$4.65 \cdot 10^{-6}$ (4.6)	0.84 (0.8)	$7.41 \cdot 10^3$ (4.7)	$1.08 \cdot 10^{-5}$ (1.2)	0.92 (0.9)	$432 \cdot 10^3$ (2.4)
Nanoperforated PLA	55.5 (3.0)	$1.95 \cdot 10^{-5}$ (7.9)	0.57 (1.6)	$1.83 \cdot 10^3$ (6.6)	$6.23 \cdot 10^{-5}$ (2.0)	0.71 (2.1)	$26.25 \cdot 10^3$ (2.9)
Omp2a-filled nanoperforated PLA	79.3 (2.5)	$1.68 \cdot 10^{-5}$ (8.9)	0.84 (2.8)	$1.87 \cdot 10^3$ (7.1)	$5.21 \cdot 10^{-4}$ (13.9)	0.53 (5.4)	$3.67 \cdot 10^3$ (8.4)
500 mM							
Non-perforated PLA	63.7 (1.0)	$4.4 \cdot 10^{-6}$ (2.8)	0.87 (0.5)	$9.39 \cdot 10^3$ (3.8)	$1.15 \cdot 10^{-5}$ (1.0)	0.91 (0.9)	$255.6 \cdot 10^3$ (1.6)

Nanoperforated PLA	32.1 (3.8)	$6.61 \cdot 10^{-5}$ (6.1)	0.48 (1.5)	$2.1 \cdot 10^3$ (10.9)	$6.72 \cdot 10^{-5}$ (2.3)	0.78 (2.0)	$26 \cdot 10^3$ (2.7)
Omp2a-filled nanoperforated PLA	54.6 (2.2)	$3.32 \cdot 10^{-5}$ (10.4)	0.79 (3.3)	751 (9.6)	$7.07 \cdot 10^{-4}$ (9.0)	0.53 (6.5)	$3.71 \cdot 10^3$ (9.0)
1000 mM							
Non-perforated PLA	42.8 (1.3)	$5.09 \cdot 10^{-6}$ (3.9)	0.87 (0.8)	$4.92 \cdot 10^3$ (5.7)	$1.34 \cdot 10^{-5}$ (1.3)	0.87 (1.2)	$117 \cdot 10^3$ (1.7)
Nanoperforated PLA	23.73 (2.7)	$1.14 \cdot 10^{-4}$ (5.9)	0.45 (1.4)	448 (3.6)	$6.97 \cdot 10^{-5}$ (0.6)	0.78 (0.4)	$21.64 \cdot 10^3$ (0.8)
Omp2a-filled nanoperforated PLA	37.6 (2.6)	$5.41 \cdot 10^{-5}$ (18.3)	0.85(4.7)	238.7 (10.8)	$6.53 \cdot 10^{-4}$ (3.9)	0.47 (2.3)	$4.22 \cdot 10^3$ (6.7)

Table S4. Resistances (R) and constant phase elements (CPE) for each sample from fitting parameters obtained with the EEC displayed in Figure 5e. For each system impedance parameters are displayed according to the CaCl₂ concentrations of 50, 100, 500 and 1000 mM. The percentage errors associated to each circuit element have been included in parentheses.

	R_S ($\Omega \cdot \text{cm}^2$)	CPE_M ($\text{Fcm}^{-2} \cdot \text{s}^{n-1}$)	n	R_M ($\Omega \cdot \text{cm}^2$)	CPE_{dl} ($\text{Fcm}^{-2} \cdot \text{s}^{n-1}$)	n	R_I ($\Omega \cdot \text{cm}^2$)
50 mM							
Non-perforated PLA	157 (0.9)	$4.3 \cdot 10^{-6}$ (5.2)	0.85 (3.6)	$9.24 \cdot 10^3$ (1.4)	$1.13 \cdot 10^{-5}$ (0.9)	0.57 (3.0)	$461 \cdot 10^3$ (4.1)
Nanoperforated PLA	112.8 (0.6)	$2.947 \cdot 10^{-5}$ (3.6)	0.82 (1.6)	$3.85 \cdot 10^3$ (13.1)	$4.14 \cdot 10^{-5}$ (2.9)	0.81 (1.9)	$52.6 \cdot 10^3$ (2.4)
Omp2a-filled nanoperforated PLA	84.8 (1.4)	$1 \cdot 10^{-4}$ (8.4)	0.61 (2.1)	$1.01 \cdot 10^3$ (17.1)	$8.2 \cdot 10^{-5}$ (2.2)	0.8 (2.2)	$16.31 \cdot 10^3$ (3.0)
100 mM							
Non-perforated PLA	115.3 (0.7)	$4.2 \cdot 10^{-6}$ (8.3)	0.6 (4.2)	$7.41 \cdot 10^3$ (2.1)	$1.15 \cdot 10^{-5}$ (0.3)	0.82 (0.8)	$410 \cdot 10^3$ (0.8)
Nanoperforated PLA	91 (0.7)	$3.67 \cdot 10^{-5}$ (1.0)	0.81 (1.1)	$1.15 \cdot 10^3$ (11.2)	$4.06 \cdot 10^{-5}$ (1.0)	0.81 (1.7)	$55.5 \cdot 10^3$ (1.7)
Omp2a-filled nanoperforated PLA	61.4 (2.0)	$8.98 \cdot 10^{-5}$ (12.4)	0.59 (2.8)	768 (16.2)	$8.52 \cdot 10^{-5}$ (2.8)	0.83 (2.6)	$12.14 \cdot 10^3$ (3.4)
500 mM							
Non-perforated PLA	58.21 (1.0)	$3.5 \cdot 10^{-6}$ (2.0)	0.92 (0.2)	$8.21 \cdot 10^3$ (1.4)	$1.41 \cdot 10^{-5}$ (3.0)	0.87 (0.9)	$197.5 \cdot 10^3$ (1.5)

Nanoperforated PLA	60.5 (0.9)	$7.75 \cdot 10^{-5}$ (13.0)	0.77 (2.8)	326 (15.8)	$4.07 \cdot 10^{-5}$ (0.9)	0.81 (0.8)	$52.4 \cdot 10^3$ (1.5)
Omp2a-filled nanoperforated PLA	41.2 (1.2)	$7.73 \cdot 10^{-5}$ (9.7)	0.68 (1.9)	246.2 (6.2)	$8.43 \cdot 10^{-5}$ (0.9)	0.81 (0.7)	$18.02 \cdot 10^3$ (1.2)
1000 mM							
Non-perforated PLA	44.8 (3.1)	$4.55 \cdot 10^{-6}$ (1.3)	0.9 (0.9)	$3.92 \cdot 10^3$ (5.0)	$1.48 \cdot 10^{-5}$ (1.6)	0.79 (1.4)	$127 \cdot 10^3$ (4.2)
Nanoperforated PLA	53.2 (1.2)	$2.33 \cdot 10^{-4}$ (12.2)	0.61 (2.8)	411 (27.2)	$4.29 \cdot 10^{-5}$ (0.9)	0.81 (0.9)	$48.6 \cdot 10^3$ (1.4)
Omp2a-filled nanoperforated PLA	32.8 (1.1)	$1.86 \cdot 10^{-4}$ (9.3)	0.61(2.0)	196.9 (8.4)	$8.34 \cdot 10^{-5}$ (3.9)	0.81 (0.6)	$16.86 \cdot 10^3$ (1.0)

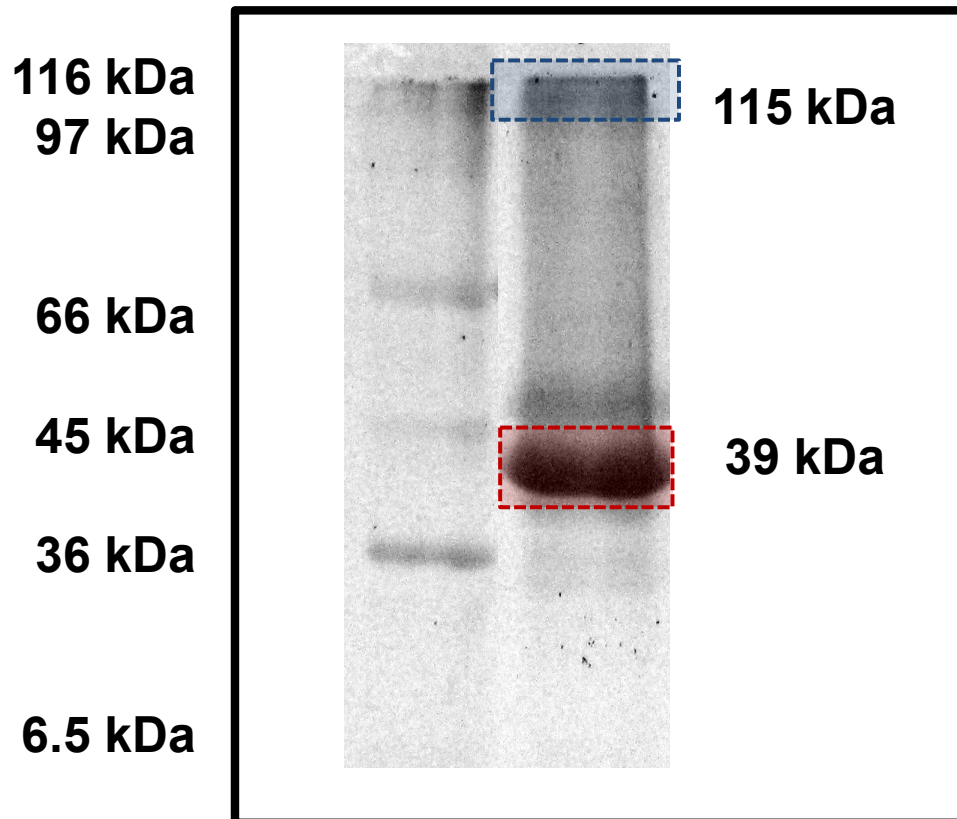


Figure S1. SDS-PAGE of Omp2a. Monomers migrate at 39 kDa while trimers show an apparent molecular weight of 115 kDa.

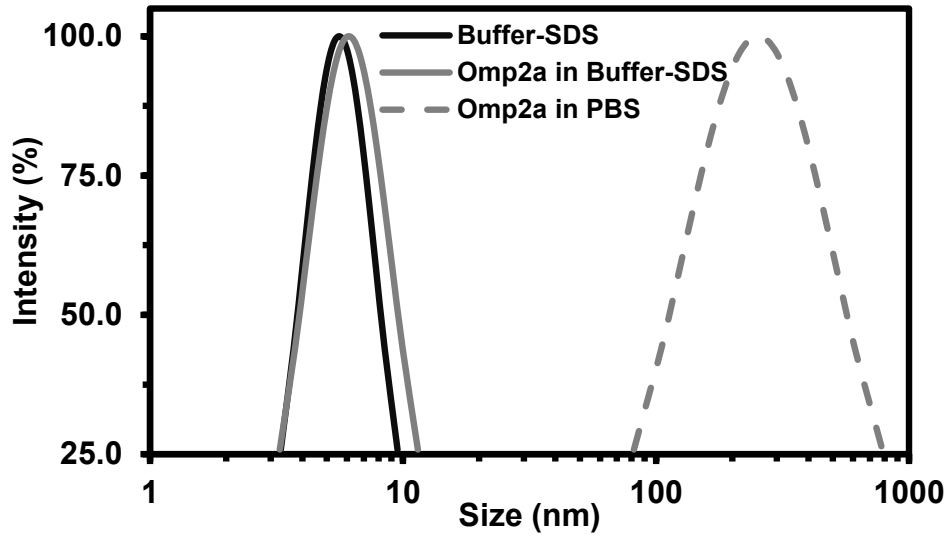


Figure S2. DLS results showing the volume percentage of particles towards particle diameter for SDS micelles in the buffer solution used to maintain the protein, the same solution after incorporate the Omp2a protein and a PBS solution with Omp2a.

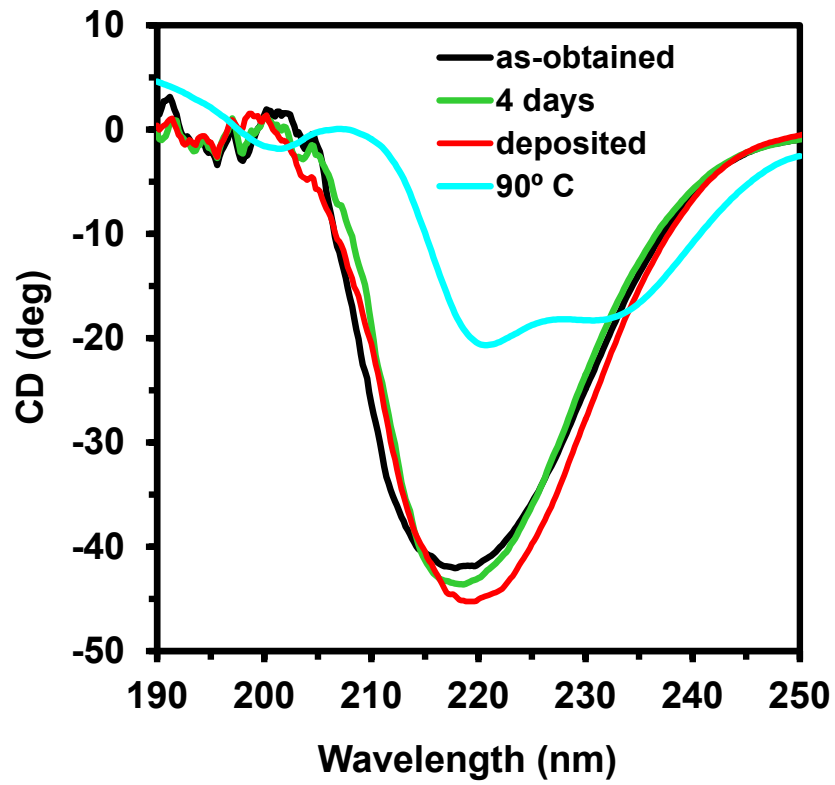


Figure S3. CD spectra for the Omp2a protein: heated 5 min at 90 °C, as-obtained, after 4 days of incubation and deposited into the nanoporations of PLA NMs.

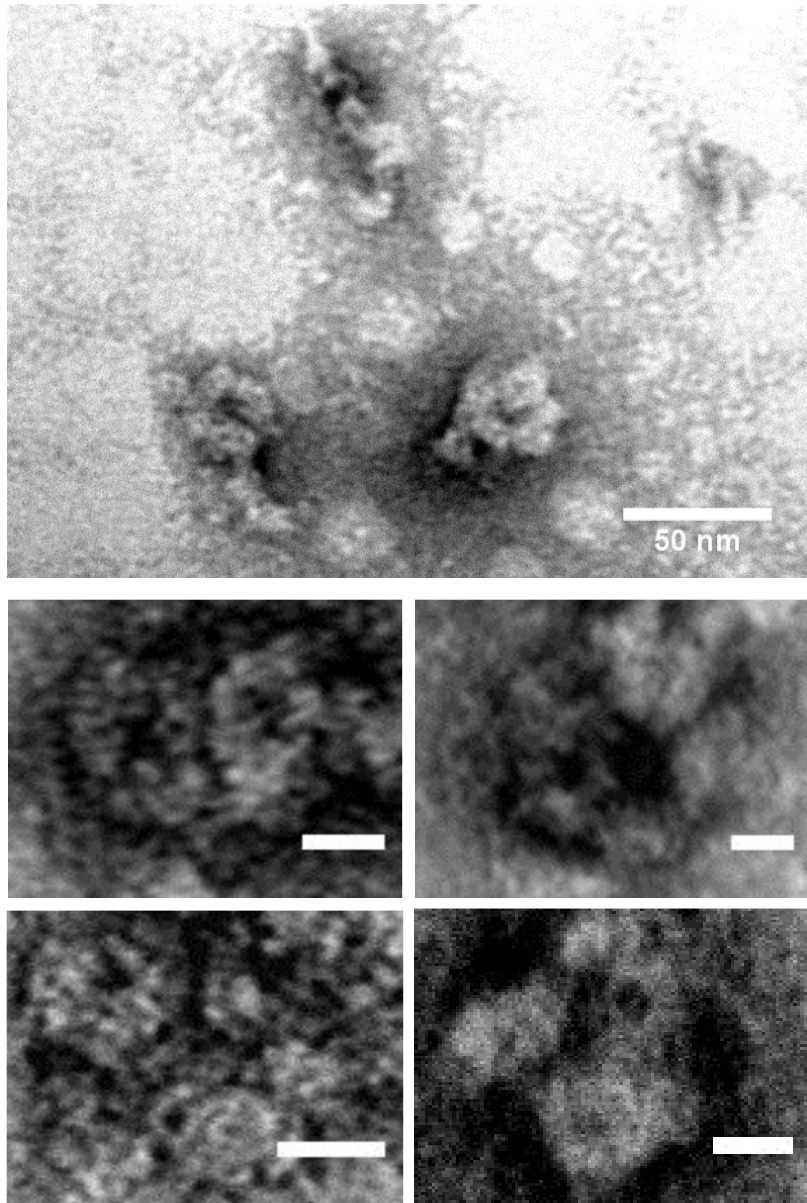


Figure S4. TEM micrographs of Omp2a trimeric units and higher aggregates derived solutions stained with 2% uranyl acetate. Scale bar of the high magnification micrographs: 10 nm.

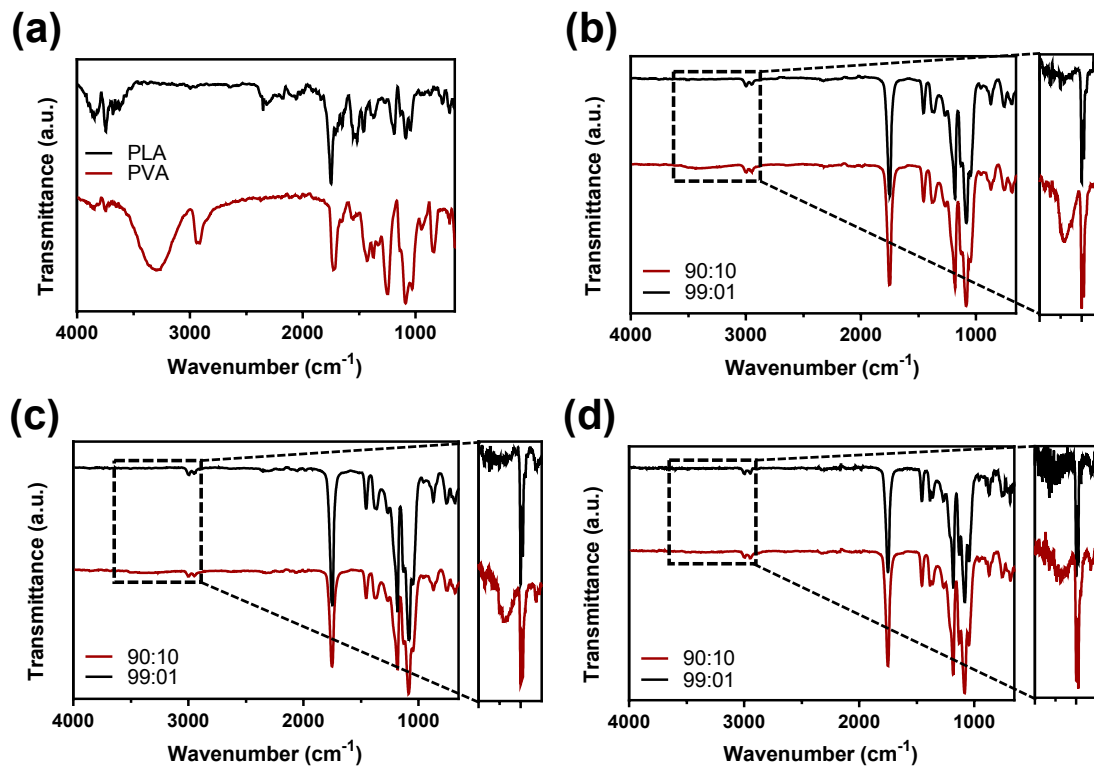
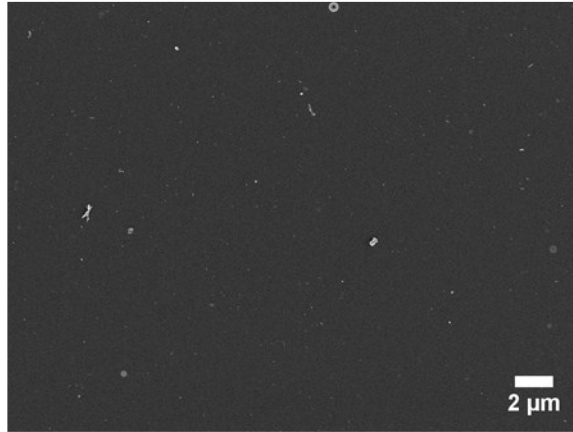


Figure S5. FTIR spectra of: (a) individual PLA and PVA membranes; (b) as prepared membranes obtained by solvent casting 99:10 and 99:1 PLA:PVA mixtures; (c) membranes of (b) after 2 h in milliQ water; and (d) membranes of (b) after one day in milliQ water.

(a)



(b)

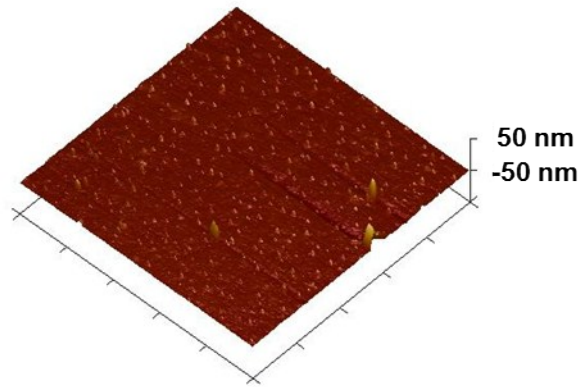


Figure S6. (a) SEM micrograph and 3D AFM height image ($5 \times 5 \mu\text{m}^2$) of non-perforated PLA NMs.

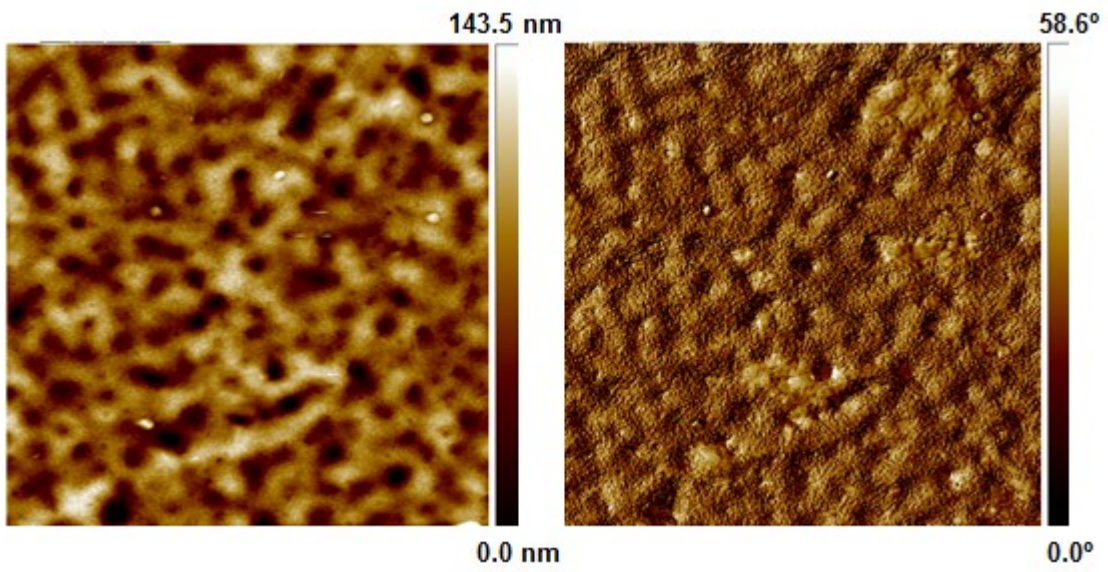


Figure S7. AFM height and their corresponding phase images (window: $5.0 \times 5.0 \mu\text{m}^2$) of nanoporous PLA after Omp2a deposition.

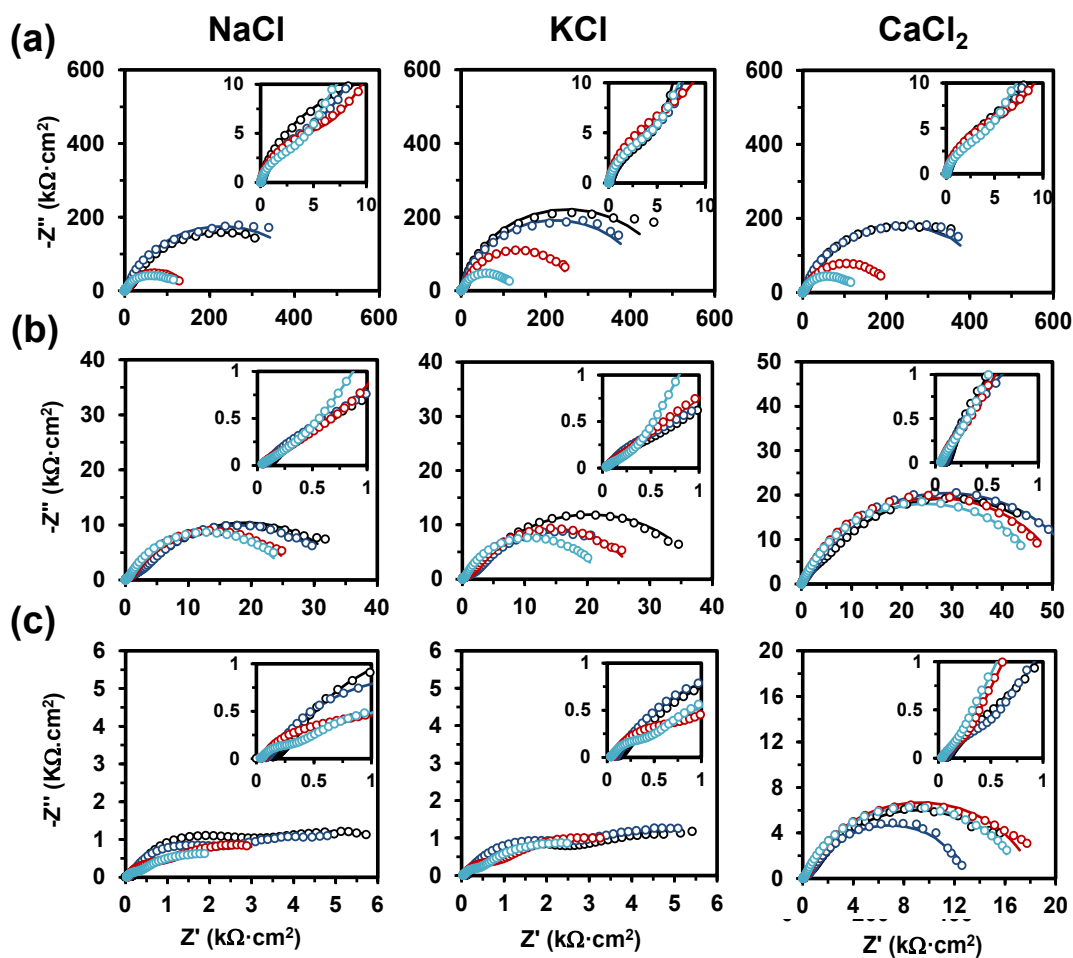


Figure S8. Nyquist plots of (a) non-perforated, (b) nanoporated and (c) Omp2a-filled nanoporated PLA NMs in NaCl, KCl and CaCl₂ aqueous solutions at 50, 100, 500 and 1000 mM concentrations (black, dark blue, red and light blue profile, respectively). Symbols correspond to experimental data, while lines are the fittings to the corresponding electrical equivalent circuit (EEC) displayed in Figure 5e.

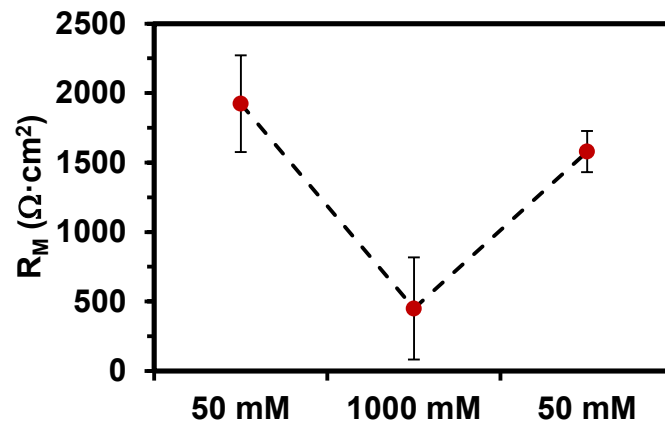


Figure S9. Variation of the Omp2a-filled nanoporated membrane resistance (R_M) with the KCl concentration. The values are the mean of three samples and their standard deviation.